

Supporting Information for Manuscript

A Block Copolymer Templated Approach for the Preparation of Nanoporous Polymer Structures and Cellulose Fiber Hybrids by Ozone Treatment

Lea Gemmer¹, Qiwei Hu^{2,5}, Bart-Jan Niebuur³, Tobias Kraus^{3,4}, Bizan N. Balzer^{2,5,6},

Markus Gallei^{1,7}*

¹Chair in Polymer Chemistry, Universität des Saarlandes, Campus Saarbrücken C4 2, 66123 Saarbrücken, Germany

²Institute of Physical Chemistry, University of Freiburg, Albertstr. 21, 79104 Freiburg, Germany

³INM-Leibniz-Institute for New Materials, Campus D2 2, 66123 Saarbrücken, Germany

⁴Colloid and Interface Chemistry, Universität des Saarlandes, Campus D2 2, 66123 Saarbrücken, Germany

⁵Cluster of Excellence livMatS @ FIT-Freiburg Center for Interactive Materials and Bioinspired Technologies, University of Freiburg, Georges-Köhler-Allee 105, 79110 Freiburg, Germany

⁶Freiburg Materials Research Center (FMF), University of Freiburg, Stefan-Meier-Str. 21, 79104 Freiburg, Germany

⁷Saarene, Saarland Center for Energy Materials and Sustainability, Campus Saarbrücken C4 2, 66123 Saarbrücken, Germany

Block Copolymer Synthesis and Film Casting

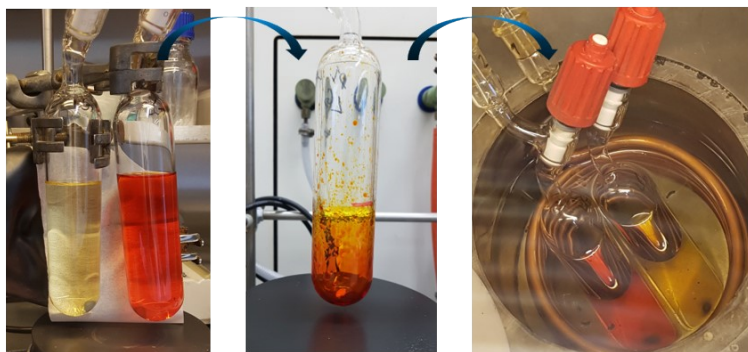


Figure S1: Photographs of sequential anionic synthesis of PI-*b*-P2VP block copolymer. Left: living PI anions in cyclohexane before and during endcapping with DPE. Middle: living PI-DPE anions after removal of the solvent. Right: PI-DPE in THF before and after addition of second monomer 2VP.

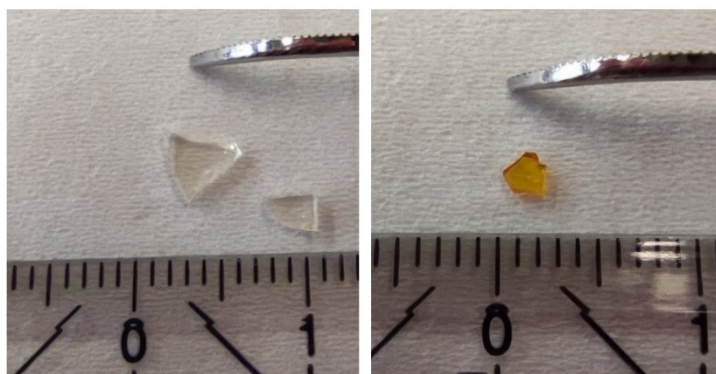
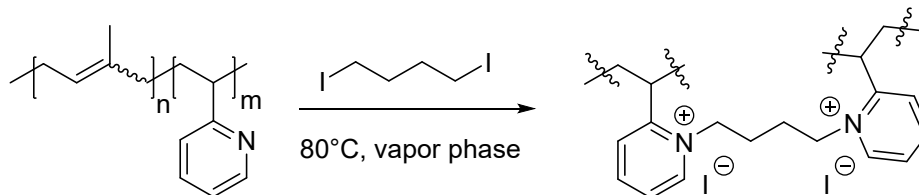


Figure S2: Photographs of bulk films of PI₂₈-*b*-P2VP₇₂⁶³. Left: untreated; Right: after stabilizing with DIB.



Scheme S1: Proposed chemical structure of DIB-crosslinked pyridine moieties in PI-*b*-P2VP block copolymer.

Water content of P2VP homopolymer and $\text{PI}_{28}\text{-}b\text{-P2VP}_{72}^{63}$ block copolymer

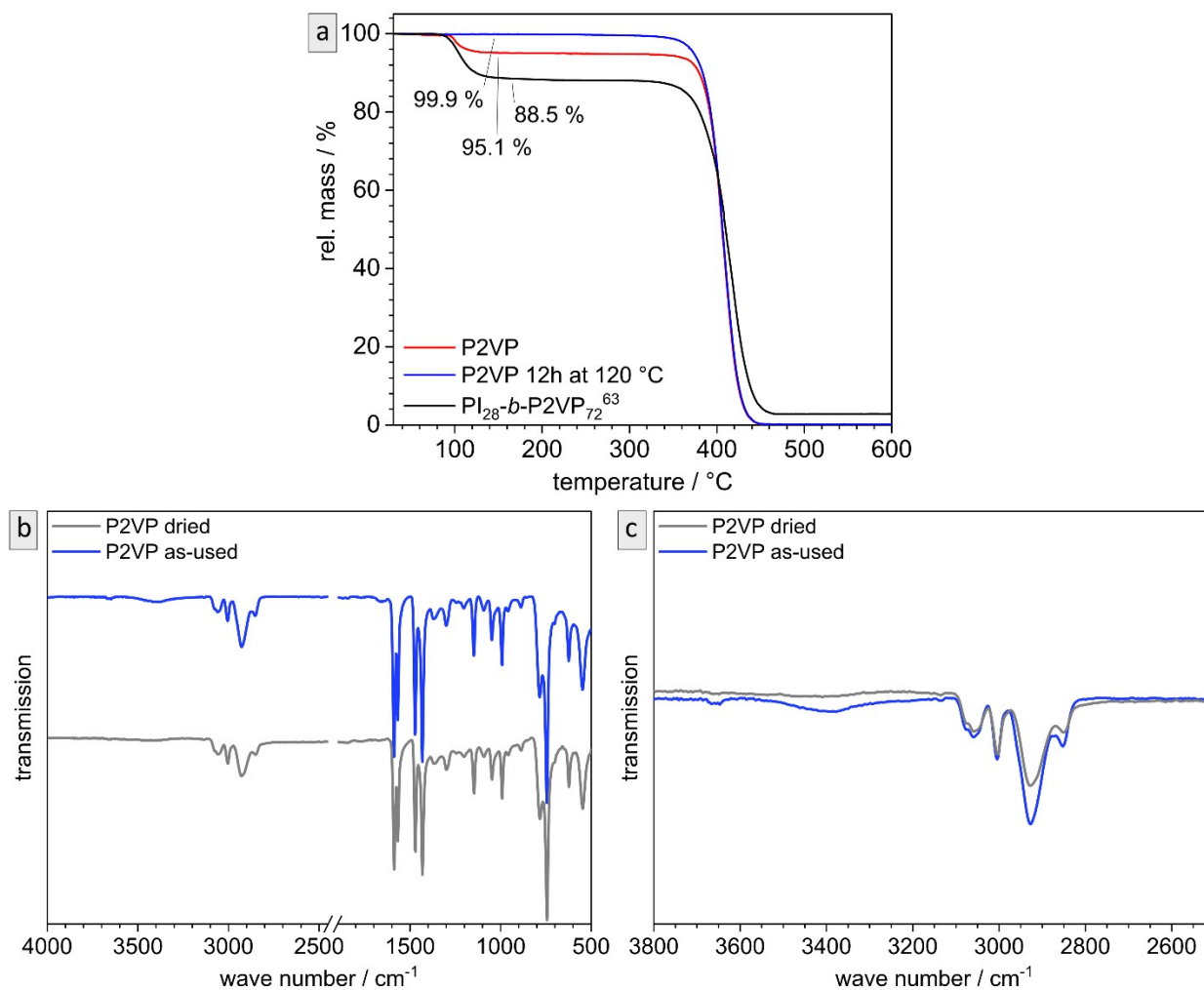


Figure S3: TGA (a) and FTIR (b and c) measurements of $\text{PI}_{28}\text{-}b\text{-P2VP}_{72}^{63}$ BCP, and P2VP homopolymer before and after drying.

EDS point measurements on bulk samples

Table S1: Concentrations of selected atoms in PI₂₈-*b*-P2VP₇₂⁶³ bulk sample determined via EDS point measurements at 8 kV. Values are calculated from four to five single spectra with the referred distance from the edge.

| Location | Distance from edge ^{a)} | Iodine | | Oxygen | | Chlorine | | Nitrogen | |
|----------|----------------------------------|-----------|----------|-----------|----------|-----------|----------|-----------|----------|
| | | \bar{X} | σ | \bar{X} | σ | \bar{X} | σ | \bar{X} | σ |
| | / μm | / atm-% | | | | | | | |
| c | 0.3 – 0.5 | 2.2 | 0.2 | 2.9 | 0.6 | - | - | 9.2 | 1.2 |
| d | 2 – 3 | 2.1 | 0.7 | 1.0* | - | 0.2* | - | 8.9 | 1.0 |
| e | 8 – 10 | 0.4 | < 0.1 | 0.6 | 0.6 | 1.2 | 0.4 | 9.8 | 0.9 |
| f | 25 | 0.0 | 0 | 0.7 | 0.4 | 1.8 | 0.4 | 8.5 | 0.8 |

a) Estimated from SEM-images. * Mean value deriving from only two values that could be gathered.

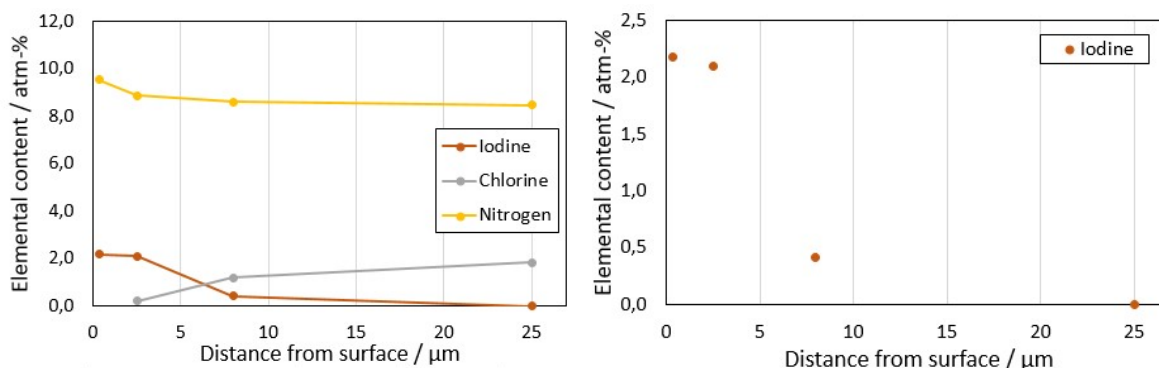


Figure S4: Plot of elemental contents in dependence of the distance to the surface, as determined via EDS.

While the iodine content was discussed in the main text and nitrogen is present everywhere in the PVP-containing polymer, chlorine and oxygen contents are shortly discussed in this section. Low concentrations of chloride were found, as can be concluded from Table S1 and the corresponding EDS investigations. A plausible source for chloride is LiCl used during sequential anionic polymerization, which it is assumed to accumulate in the amphiphilic BCP even through polymer work-up procedures. Also, low concentrations of oxygen can be found. In these EDS measurements, both the concentrations of oxygen and nitrogen feature relatively high error values. Therefore, no conclusions will be drawn from these values listed in Table S1. Additionally, background-measurements also contain 5 – 9 atm-% oxygen and therefore these values are neglected.

Using the atomic ratios of iodine from EDS, theoretical amounts of cross-linking sites can be estimated. As nitrogen atoms cannot be quantified reliably using EDS, the molecular weight as determined via MALLS-SEC as well as molar composition of the BCPs as derived from the corresponding NMR spectra were used. By this means, the atomic fraction of N can be calculated. The BCP contains 28 mol-% PI, which consists of 5 C atoms per unit, and 72 mol-% P2VP ($0.72 = x_{P2VP}$), which consists of 7 C atoms and 1 N atom per unit ($8^{-1} = x_{N,P2VP}$). Therefore, the atomic fraction of N is calculated by:

$$x_{P2VP} \cdot x_{N,P2VP} \cdot 100 \% = 0.72 \cdot 0.125 \cdot 100 \% = 9 \% \quad (S1)$$

Using all the values determined from the corresponding EDS spectra, the fraction of BCP can be considered to calculate a plausible value for nitrogen N_{calc} . Based on that, a ratio of nitrogen per iodine can be calculated. Considering the segment-length of P2VP ($D_{pn} = 475$) the number of cross-links per chain can be calculated, as compiled in TableS2.

Table S2: Correlations between nitrogen and iodine concentrations determined by theoretical calculation and EDS measurements, respectively, and the ratio thereof (N per I).

| Location | Distance from surface / μm | N_{calc} / atm-% ^{b)} | I_{EDS} / atm.-% | Fraction of N with I | CL per chain |
|----------|---------------------------------|----------------------------------|--------------------|----------------------|--------------|
| c | 25 | 8.8 | 0 | 0 | 0 |
| d | 8 – 10 | 8.7 | 0.4 | 5 | 22 |
| e | 2 – 3 | 8.7 | 2.1 | 24 | 115 |
| f | 0.3 – 0.5 | 8.4 | 2.2 | 26 | 124 |

^{b)} considering all other elemental contents found in EDS

SEM images of morphology and pore sizes of Sample Bs10a

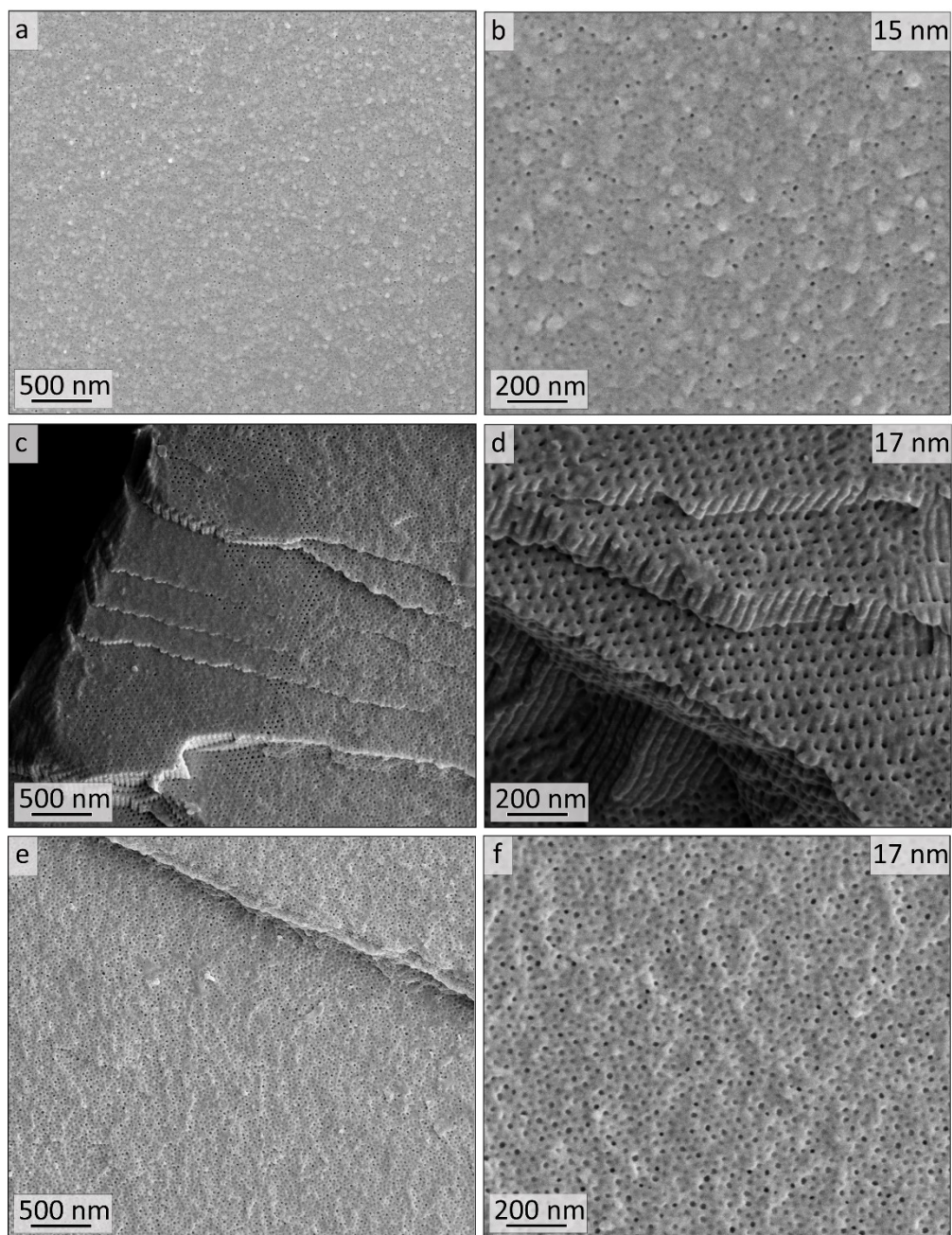


Figure S5: SEM images (inlet: mean pore diameters) of bulk polymer from $\text{PI}_{28}\text{-}b\text{-P2VP}_{72}$ ⁶³ from sample Bs10a. a) and b): in the middle of the cross-section, $\sigma = 2$ nm, c) and d): at the edge of the cross-section (near-surface area), hexagonal area, $\sigma = 2$ nm e) and f): close to the edge of the cross section, bcc area, $\sigma = 3$ nm.

FTIR of ozone-treated bulk samples

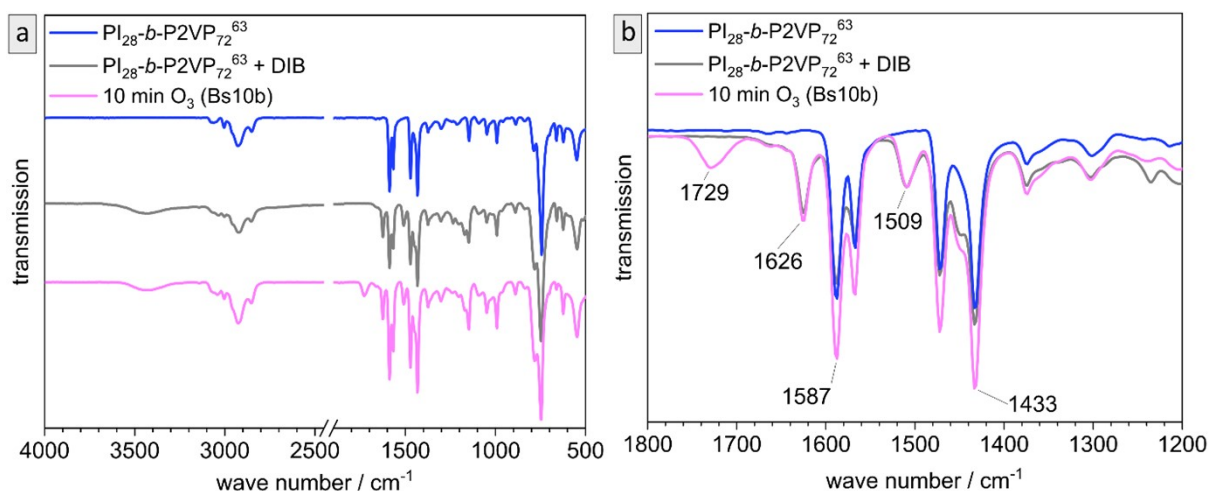


Figure S6: Analysis of untreated film ($\text{PI}_{28}\text{-b-P2VP}_{72}^{63}$, blue), DIB-crosslinked film (gray), and ozone-treated film (magenta) in ATR-FTIR transmission spectra. a) overview, whole spectrum. b) partial spectrum, changes in P2VP signals.

Extraction of carboxylic components by washing with water becomes obvious when comparing the sample washed with heptane only (Bs10a, magenta) to the sample washed with heptane and water (Bs10b). The peak at 1729 cm^{-1} corresponding to carboxylic derivatives is very dominant before washing with water and is decreased strongly afterwards.

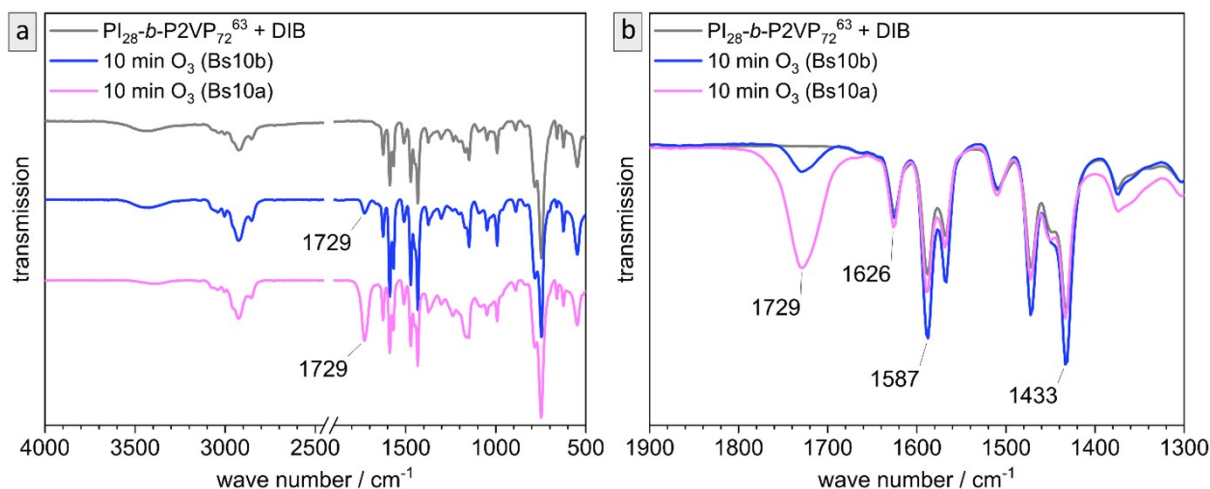


Figure S7: Comparison of initial film (gray) and to ozone-treated sample Bs10a washed with heptane only (magenta) and ozone treated sample Bs10b washed with heptane and water (blue) in ATR-FTIR transmission spectra. Left: overview, whole spectrum. Right: zoom-in on change in signals.

SEM images of BCP coating on cellulose fiber discs

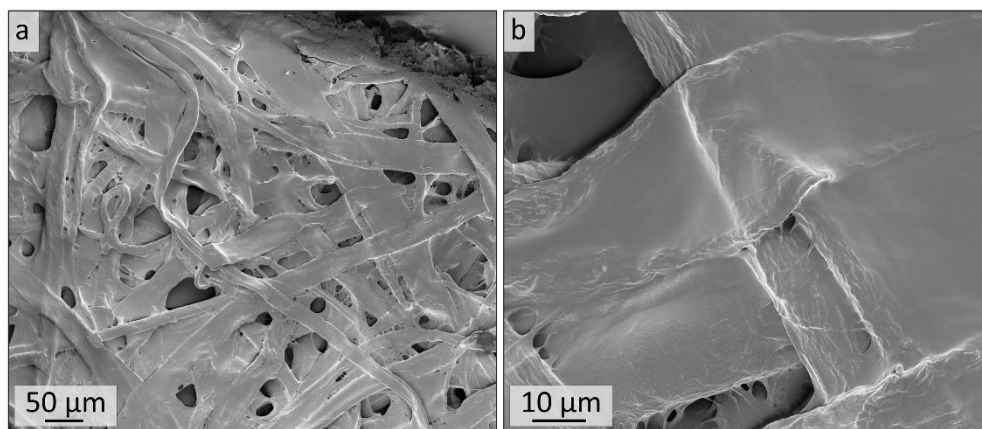


Figure S8: SEM images of the surface of untreated composite material using $\text{PI}_{35}\text{-}b\text{-P2VP}_{65}^{186}$ on Munktell cellulose-based filter discs (grade 3hw) in low magnifications. Macroporous cellulose fiber structure is retained and well-visible (compare to Fig. S9a).

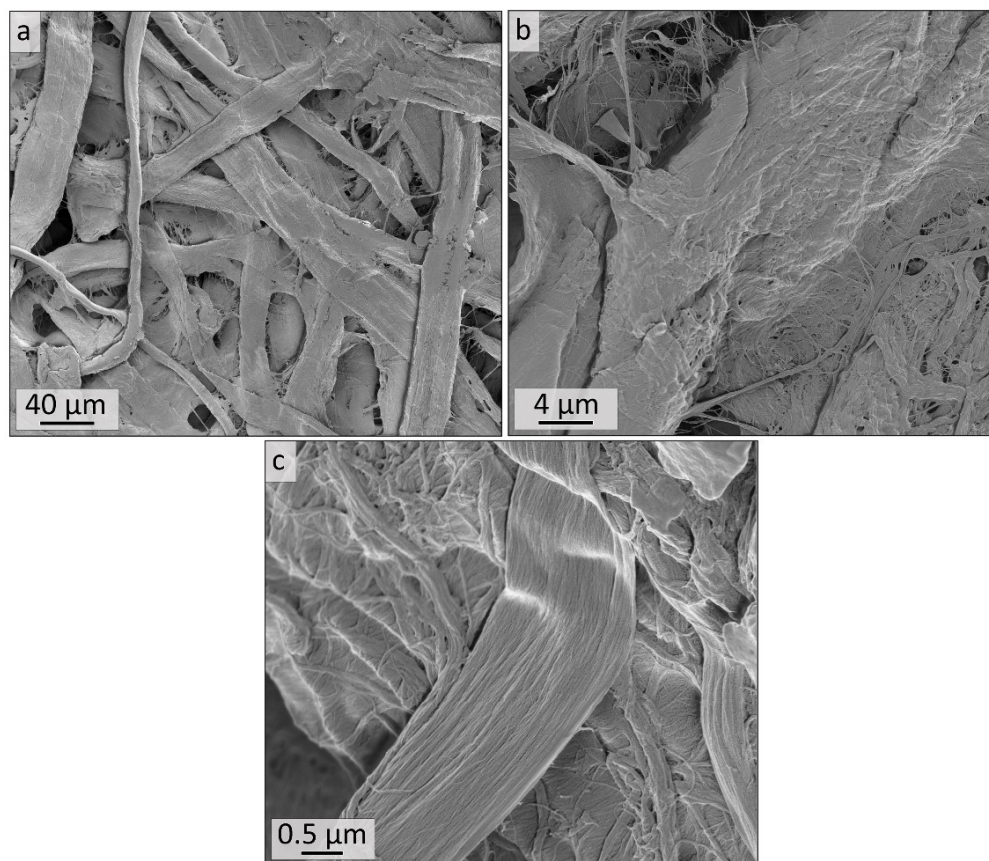


Figure S9: SEM images of the surface of untreated cellulose-based filter discs by Munktell (grade 3hw) in increasing magnifications (a – c).

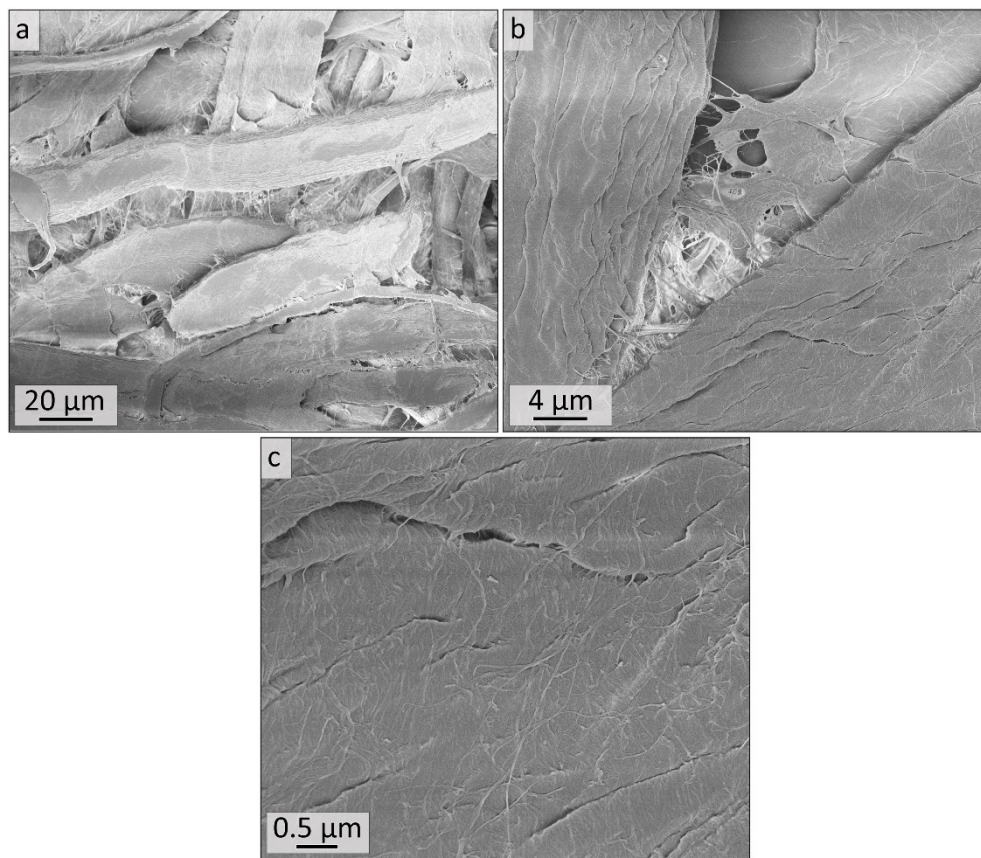


Figure S10: SEM images of the surface of cellulose-based filter discs by Munktell (grade 3hw) after treatment with ozone according to the protocol used for samples C10 and Cs10 in increasing magnifications (a – c).

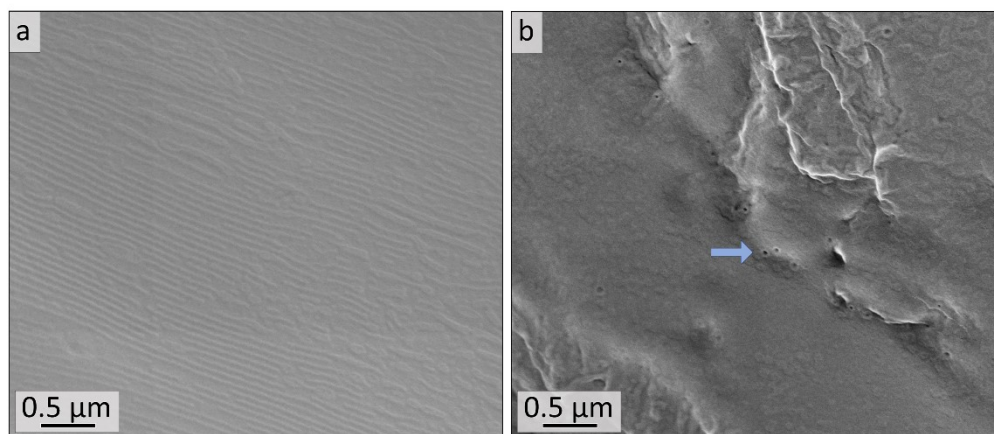


Figure S11: SEM images of the surface of untreated composite material using $\text{PI}_{35}\text{-}b\text{-P2VP}_{65}^{186}$ on Munktell cellulose-based filter discs (grade 3hw) in high magnifications. Block copolymer segment domains are visible in two different morphologies, in a) lamellae or lying cylinders and

in b) spheres or standing cylinders. The blue arrow marks an open pore that is also depicted in Fig. 8b.

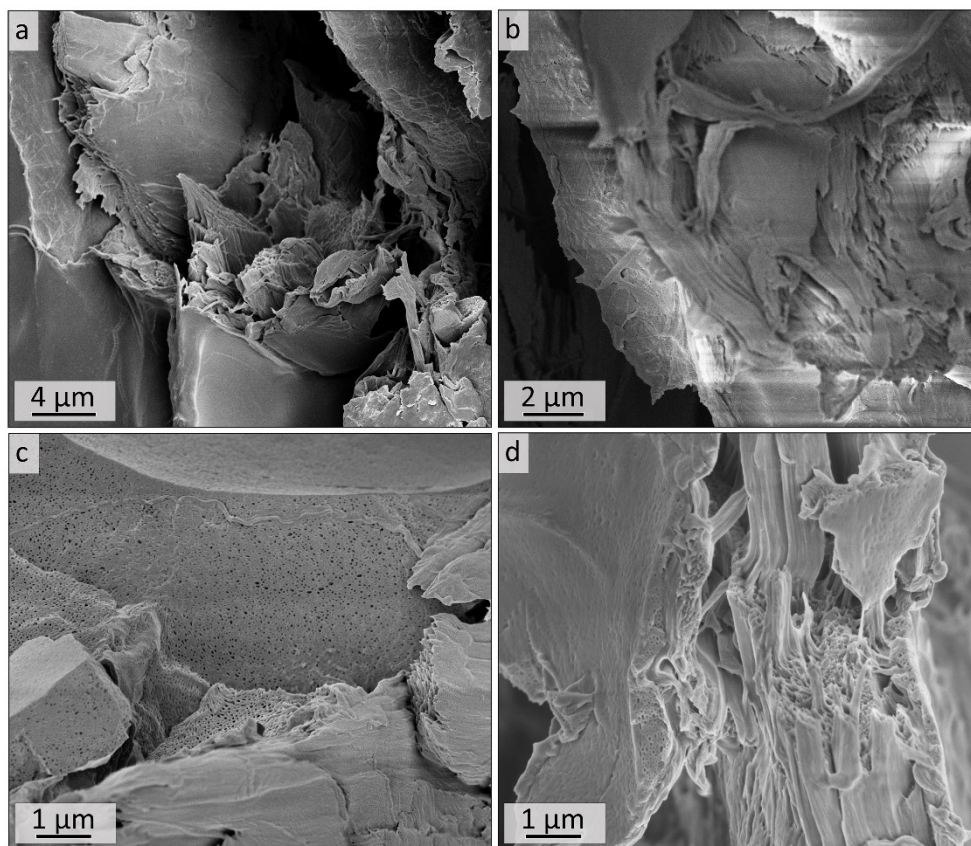


Figure S12: SEM analysis of the cross-sections of untreated (a and b) and ozone treated (sample Cs10, c and d), composite material using $\text{PI}_{35}\text{-}b\text{-P2VP}_{65}$ ¹⁸⁶ on Munktell cellulose-based filter discs. Polymer coating on cellulose fibers can be seen, as well as varying film thicknesses (images b-d).

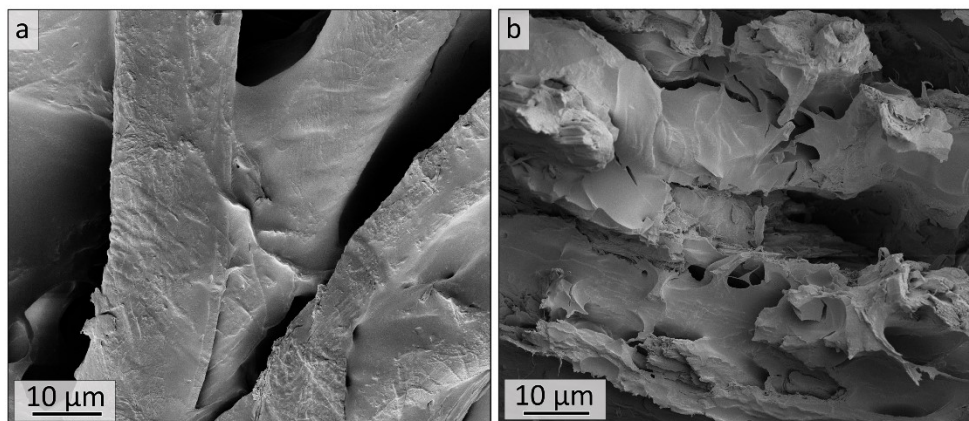


Figure S13: SEM images of the a) surface and b) cross-sections of ozone treated and acid-swollen sample Cs10 after washing and drying as overview images.

EDS point measurements on cellulose composite material

Table S3: Concentrations of selected atoms in PI₃₅-b-P2VP₆₅¹⁸⁶ coated on Munktell cellulose-based filter discs (grade 3hw) after treatment with DIB (corresponds to sample Cs10 before ozone treatment) determined via EDS point measurements at 8 kV. Values are calculated from single spectra distributed over the cross-section as it is shown in Fig. S14.

| Location | Iodine | | Oxygen | | Chlorine | | Nitrogen | |
|----------|-----------|----------|-----------|-------------------|-----------|-----------------|-----------|----------|
| | \bar{X} | σ | \bar{X} | σ | \bar{X} | σ | \bar{X} | σ |
| | / atm-% | | | | | | | |
| 1 | 3.4 | 2.0 | 4.7 | 4.3 ^{b)} | 0 | 0 | 6.3 | 1.3 |
| 2 | 2.9 | 0.7 | 5.8 | 5.7 ^{b)} | - | - ^{c)} | 7.1 | 2.2 |

- a) Estimated from SEM-images. ^{b)} Oxygen values (atm-%) vary between 1.2 and 12.9 (Location 1) and between 1.6 and 17.1 (Location 2). Since the sample substrates are cellulose fibers the deviations are accepted. ^{c)} In one out of seven spectra 0.2 atm-% chlorine is detected, 6 out of 7 do not detect chlorine.

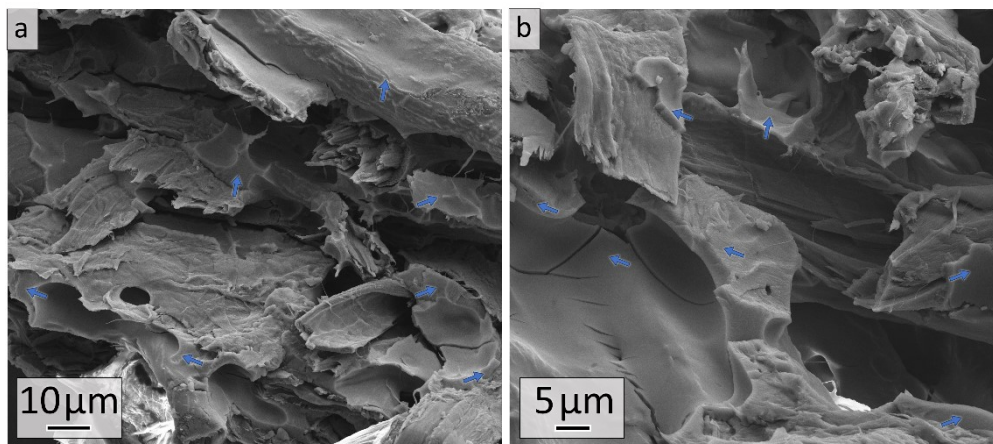


Figure S14: SEM images of cross-sections of composite sample made of PI₃₅-*b*-P2VP₆₅¹⁸⁶ on cellulose substrate via vertical deposition after stabilization with DIB. The cross-sectional image a) corresponds to location 1 in Table S3 and image b) corresponds to location 2. The exact locations of the collected EDS point spectra are marked. In image a) the two upper points are neglected in the calculation of mean values and standard deviations because no nitrogen was detected.

WCA measurements on composite materials

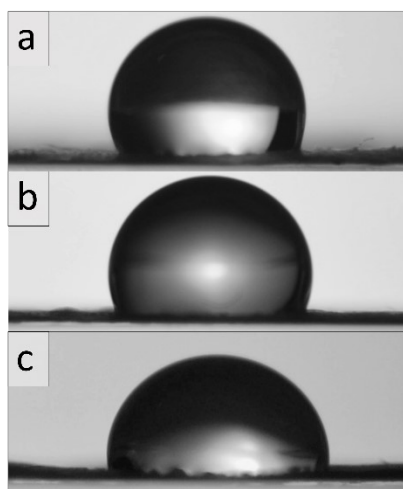


Figure S15: Photographs of WCA ($t \leq 3$ min) of a) untreated polymer-coated filter paper, $\theta = 114^\circ \pm 7$, b) DIB-stabilized polymer-coated filter paper, $\theta = 109^\circ \pm 7$ and c) ozone-treated DIB-stabilized sample Cs10, $\theta = 102^\circ \pm 9$.

Table S4: Single values of WCA measurements on cellulose fiber disc composite materials in three different spots on each sample.

| | Initial ^{a)} | | + DIB ^{b)} | | Cs10 ^{c)} | |
|------------|------------------------------|-------|----------------------------|-------|---------------------------|-------|
| | left | right | left | right | left | right |
| | WCA (Θ) / ° | | | | | |
| Location 1 | 115 | 112 | 103 | 122 | 119 | 99 |
| Location 2 | 115 | 128 | 110 | 112 | 102 | 104 |
| Location 3 | 111 | 104 | 104 | 100 | 97 | 89 |
| Mean-value | 114 | | 109 | | 102 | |
| σ | 7 | | 7 | | 9 | |

a) PI₃₅-*b*-P2VP₆₅¹⁸⁶ on paper, b) PI₃₅-*b*-P2VP₆₅¹⁸⁶ on paper after stabilization with DIB,
c) corresponding sample after ozone treatment